JPP Journal of Pharmacy and Pharmacology

JPP 2006, 58: 959–966

Received December 20, 2005
Accepted March 20, 2006
DOI 10.1211/jpp.58.7.0011
ISSN 0022-3573

A tetravalent RGD ligand for integrin-mediated cell adhesion

N. Watson, G. Duncan, W. S. Annan and C. F. van der Walle

Abstract

Monovalent RGD (arginine-glycine-aspartic acid) peptides or polymers furnished with RGD in random distributions are employed as cell-scaffolds and gene delivery vehicles. However, integrin binding to RGD is dependent on the spatial distribution (clustering) of the ligand and intrinsic integrin affinity via conformational changes (avidity). Here we have designed and expressed a polypeptide consisting of a tetrameric coiled coil and spacer facilitating polyvalent (clustered) display of integrin ligands; the RGD motif was used as proof of principle. Size-exclusion chromatography and circular dichroism showed that the polypeptide self assembled as a tetramer in solution with a defined secondary structure. Cell adhesion to surfaces coated with the polypeptide was up to 3-fold greater than that for (monovalent) RGDS peptide at equivalent concentrations. Moreover, the polypeptide in solution at concentrations $\geq 1\,\mu$M inhibited cell adhesion to fibronectin-coated surfaces, while RGDS peptide in solution at concentrations up to $500\,\mu$M did not. These cell data demonstrate that the polypeptide bound integrin receptors in a polyvalent manner. The polypeptide will therefore be of use in the engineering of tissue-culture scaffolds with increased cell adhesion activity, or to targeted gene delivery vehicles, and could incorporate protein ligands in place of the RGD motif.

Introduction

For tissue growth, organisation and repair the interaction between cells and their extracellular matrix (ECM) is critical. The ECM component involved in integrin-mediated cell adhesion is dependent upon the integrin subtype (e.g. osteoclasts bind collagen via $\alpha1\beta1$ and $\alpha2\beta1$ integrins, whereas fibroblasts bind fibronectin (FN) and vitronectin via $\alpha5\beta1$ and $\alpha v\beta3$ integrins, respectively (Humphries 2000)). The primary integrin binding motif, arginine-glycine-aspartic acid (RGD), is found in several ECM proteins, most notably, the 10^{th} type III FN domain (FIII 10) (Pierschbacher & Ruoslahti 1984). Organisation of FN fibrils in the extracellular matrix renders a polyvalent display of ligand to the cell surface, integrin-driven polymerisation of soluble FN being dependent on extension of the FN monomer to expose FN self-associating sites (Ingham et al 1997). The resultant FN fibrils are able to undergo extension/contraction over a four-fold change in length, yielding an elastic matrix (Ohashi et al 1999). Such dynamic movements within the cell matrix inevitably change both the matrix rigidity and the spatial arrangement of the ligand display seen by the cell. Interestingly, fibroblasts have been shown to probe the elasticity of their supporting matrix, responding to greater elasticity with increased motility and protruding lamellipodia but decreased spread morphology (Pelham & Wang 1997).

Cell responses to increased matrix rigidity can be accounted for, at least in part, by a proportional strengthening of the links between integrins and the cytoskeleton (adhesion reinforcement) (Choquet et al 1997). However, cell–FN interaction is not solely regulated by adhesion reinforcement. Electron microscopy techniques have also demonstrated large conformational changes of the integrin receptor and thereby a mechanism by which control of the intrinsic binding affinity of integrins can be controlled (Carman & Springer 2003).

Pharmaceutical Sciences, Institute for Biomedical Sciences, University of Strathclyde, Glasgow, UK

N. Watson, G. Duncan, W. S. Annan, C. F. van der Walle

Correspondence: C. F. van der Walle, Pharmaceutical Sciences, Institute for Biomedical Sciences, University of Strathclyde, Glasgow, UK. E-mail: chris.walle@strath.ac.uk

Acknowledgement and funding: This work was supported by the Wellcome Trust, grant number 067390/Z/02/Z. We are indebted to Thomas Jess and Prof. Nicholas Price, Scottish Circular Dichroism Facility, University of Glasgow, UK, for analysis and helpful discussions.

Further, a direct relationship between RGD organisation and cell behaviour has been observed, cell migration and actin polymerisation being greater on polymeric surfaces presenting RGD combs of 3.6–5.4 over combs of 1.7 (Maheshwari et al 2000; Koo et al 2002). As a result, questions must now be raised over previous results for minimal RGD densities required to support cell adhesion and spreading because these were based on random ligand distributions (Massia & Hubbell 1991). This has important consequences for the engineering of tissue supports that, to date, generally involves RGD conjugation to polymers in a random distribution or non-specific adsorption of collagen or fibronectin (Rowley et al 1999; Tan et al 2001; Yang et al 2001). Similarly, recombinant proteins and polypeptides binding integrin for targeted gene delivery via receptor-mediated endocytosis have focussed on monovalent RGD and invasin ligands, extended by cationic polypeptides binding DNA (Harbottle et al 1998; Fortunati et al 2000; Kunath et al 2003). As our understanding of integrin–ligand binding advances, it would appear timely to explore alternative polypeptide templates facilitating a clustered organisation of RGD ligands. Such polypeptides could show good potential when adapted into the construction of tissue engineering scaffolds or for the targeting of gene delivery vehicles to cells expressing integrin receptors on their apical surface.

To this aim, we describe the design and construction of a tetrameric polypeptide, self-assembling via a coiled coil domain from the tetrabrachion protein and thereby enabling polyvalent RGD–integrin binding. A coiled coil domain was used since these α-helical peptides motifs form stable parallel or antiparallel oligomers with left- or right-handedness according to their amino acid sequence (Harbury et al 1998). The coiled coil domain of tetrabrachion consists of undecapeptide repeats forming a right-handed, parallel four-stranded rod (Peters et al 1995; Stetefeld et al 2000). This parallel arrangement of the helices was required to present the appended RGD ligand in one orientation for cell surface integrin binding. Since RGD combs of 3.6–5.4 were shown to improve cell motility on polymeric support (Koo et al 2002), RGD clusters of four are appropriate to the study here. Tetrabrachion therefore represents a useful choice to promote polyvalency since it has a tetrameric parallel coiled coil arrangement (Stetefeld et al 2000). The steric hindrance anticipated between neighbouring integrins on multiple binding was addressed using a spacer between the coiled coil and RGD ligand. For an integrin diameter of ~100 Å, a duplicated primitive IgG hinge (a highly conserved 15 amino acid sequence (Michaelsen et al 1977)) was considered sufficient given that the 24 amino acid IgG2A structural hinge is highly flexible and extends over 50 Å (Harris et al 1997). The resultant polypeptide assembly, coiled coil-hinge-RGDS (Figure 1), was expressed as an N-terminal polyhistidine fusion in *Escherichia coli* and is referred to as the polypeptide in the following text. It should be noted that Figure 1 is a cartoon describing the self assembly process and should not be taken as an accurate model of the relative orientations of the RGDS ligand or mobility of the hinge region in solution.

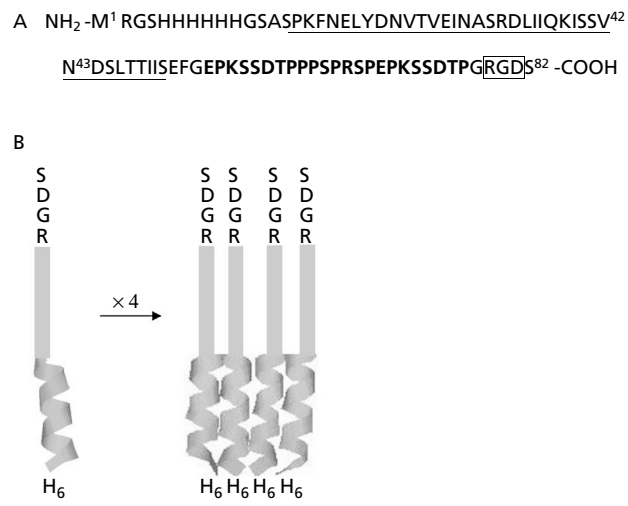

Figure 1 A. Amino acid sequence of the polypeptide expressed as the polyhistidine fusion product. The Pro^{1160}–Ser^{1196} tetrabrachion fragment is underlined, the IgG-like hinge is shown in bold (note that serine residues are substituted for cysteine) and the RGD motif is boxed. B. Cartoon of polypeptide tetramerisation directed by self-assembly of the coiled coil domain.

Materials and Methods

Materials

Unless otherwise specified, general chemical reagents were sourced from Sigma (Dorset, UK) or from Fisher Scientific (Leicestershire, UK), at analytical standard or equivalent quality. Oligonucleotide primers were ordered from Invitrogen (Paisley, UK) and restriction enzymes from New England Biolabs (Hertfordshire, UK).

Cloning and construction of the cDNA cassette

The cDNA of the Pro^{1160}–Ser^{1196} coiled coil fragment of tetrabrachion (GenBank accession No. U57967) was amplified from *Staphylothermus marinus* genomic DNA (DSMZ No. 3639; DSMZ GmbH, Braunschweig, Germany) by standard polymerase chain reaction (PCR) protocols using the forward primer CGGGATCCGCTAGCCCGAAGTTTAA TGAACTATATGA and the reverse primer CCAAGCTTG AATTCACTAATAATTGTTGTTAATGAATCA (all primers are shown 5′ to 3′). The PCR product was digested with BamH*I* and EcoR*I* and cloned into similarly digested pBluescript KS (Stratagene, Amsterdam, Netherlands). The hinge-RGD cassette was constructed using recursive PCR (Prodromou & Pearl 1992) with primers GATGAATTCG GTGAACCGAAATCTTCTGACACCCCGCCACCGTC TCCGCGTTCTCCGGAGCCAAAGTCC and ATCAAG CTTCTCGAGTTAGGAGTCACCACGACCCGGAGTA TCGzGAGGACTTTGGCTCCGGAGAACGCGG, having a 24-base central overlap. The recursive PCR product

was digested with EcoR*I* and Hind*III* and cloned upstream of the cloned Pro^{1160}–Ser^{1196} cDNA in pBluescript, similarly digested with EcoR*I* and Hind*III*. To facilitate expression of the recombinant gene in *E. coli*, the full-length cDNA cassette in pBluescript was excised with BamH*I* and Hind*III* and subcloned into pQE80-L (Qiagen, Sussex, UK), termed pQE80-CCRGD. To verify that binding between cell integrin receptors and the polypeptide occurred via the RGD motif, the control (non-binding) RGE motif was constructed by site directed mutagenesis of pQE80-CCRGD, using mutagenic primers ACTCCGGGTCGTGGTGAGTCCTAACTCGA GAAGCT and AGCTTCTCGAGTTAGGACTCACCAC GACCCGGAGT and the Quikchange protocol (Stratagene). All cloned DNA sequences were verified on a PE ABI 377 DNA Sequencer using dRhodamine Dye Terminator chemistry.

Expression and purification of the polypeptide

E. coli DH5α cells were transformed with pQE80-CCRGD (or the RGE mutant construct) and grown at 37°C in Lennox broth containing 100 μg mL^{-1} ampicillin. On reaching an OD_{600} of 0.6, protein expression was induced with 0.1 mM isopropyl β-D-1-thiogalactopyranoside and the cells harvested 3 h later (yield $\sim$3 g L^{-1}). The histidine-tagged polypeptide was isolated by Ni^{2+}-chelation affinity chromatography, following the manufacturer's protocol (Qiagen) with an added 70 mM imidazole washing step before elution from the column with 250 mM imidazole. Eluted polypeptide was concentrated in an Amicon stirred cell with a 3000 MW cut-off membrane and further purified on a 300-mL XK26 column packed with Superdex 75 resin (Amersham Biosciences, Buckinghamshire, UK) and equilibrated in 10 mM NaH_2PO_4, 50 mM NaCl, pH 7 (phosphate buffer). Polypeptide purity and M_r (relative molecular mass) were assessed by Coomassie staining of sodium dodecyl sulfate (SDS)-polyacrylamide gels and protein concentrations were determined from A_{280} values with a calculated molar extinction coefficient (ε) of 1280 M^{-1} cm^{-1} for the polypeptide.

Characterisation of the polypeptide

The M_r of the tetramer was determined by size-exclusion chromatography, calibrating a Superdex 75 HR 10/30 column (Amersham Biosciences) with human serum albumin (Sigma A9511), ovalbumin (Sigma A7642), FIII 9-10, myoglobin equine heart (Sigma M1882) and FIII 10, equilibrated in phosphate buffer and eluted over a flow rate of 0.5 mL min^{-1}. FIII 9–10, the 9^{th} to 10^{th} type III FN domain pair, and FIII 10 were expressed and purified as previously described (Altroff et al 2001). A 50-μL volume of polypeptide, 0.8 mM, was injected onto the column and eluted as above.

Mass spectrometry characterisation was undertaken at the University of Glasgow Functional Genomics Facility by trypsin digest of the corresponding polypeptide band excised from a Coomassie-stained gel and MALDI-TOF analysis.

Conformational analysis

Circular dichroism (CD) spectra were recorded at 20°C using a Jasco J810 spectropolarimeter for the polypeptide in the far UV region, from 260 to 190 nm. Polypeptide sample was studied at a concentration of 0.8 mM with a 0.02 cm path length cell. Spectra represent an average of 8 scans, run at 50 nm min^{-1} with a 0.5 s time constant. Protein concentrations were calculated as above.

Cell culture

L929 fibroblasts (mouse, connective tissue) and HeLa cells (human, epithelial) were used between passage numbers 20 and 50. Cells were grown in Dulbecco's modified Eagle's minimum essential medium with 10% fetal calf serum (Invitrogen), 2 mM L-glutamine and 1% non essential amino acids, in 25-cm^2 polystyrene flasks (Corning) and incubated at 37°C and 5% CO_2 in a humidified incubator.

Cell functional assays

For cell adhesion assays, 100 μL of a 100 μg mL^{-1} solution of either FN, or the peptide arginine-glycine-aspartic acid-serine (RGDS), or the polypeptide, was added to column 1 wells of a 96-well flat bottomed polystyrene plate (TPP), with doubling dilutions made through to column 11 (column 12, control) and left overnight at 4°C. Wells were washed three times in phosphate-buffered saline (PBS), blocked with 1% w/v bovine serum albumin (BSA) for 1 h at 37°C and washed again. A sub-confluent layer of cells were detached with trypsin, harvested and washed in warm sterile PBS. Cells were diluted to 10^5 mL^{-1} in serum-free medium and rested for 5 min. One-hundred microlitres of the cell suspension was added to each well and the plate incubated at 37°C and 5% CO_2. After 1 h, non-adherent cells were gently washed off in warm PBS and the adherent cells fixed with 4% glutaraldehyde–4% formaldehyde in PBS. Cells were stained with 0.1% crystal violet, excess stain washed off and the remaining dye was solubilized in 200 μL methanol and read at a wavelength of 570 nm in a plate reader. The value of maximum cell adhesion (100%) was taken as the highest cell adhesion response observed to a particular immobilised ligand concentration.

For the inhibition of cell adhesion assay, a sterile 96-well flat bottomed polystyrene plate was coated with 10 μg mL^{-1} (0.05 μM) FN, washed and blocked as above and equilibrated in serum-free medium (30 μL per well) at 37°C in 5% CO_2. On the day of the assay, 100 μL of RGDS (1 mM) or polypeptide (80 μM) was added to column 1 wells of a 96-well v-bottomed plate (Nunc; v-wells were used to allow easier mixing with the cells), with doubling dilutions made as above. Cells were prepared as above and 50 μL of the cell suspension was added to each v-well and mixed. The mixture from each v-well was transferred to the FN-coated 96-well flat-bottomed polystyrene plate containing 30 μL medium. Cell clumps were gently dispersed and plates incubated for 2 h. Adherent

cells were washed, fixed and measured as above. Cell adhesion is reported as the percentage of that observed in the absence of soluble polypeptide (column 12 wells). Performing non-specific binding assays for these experiments is therefore not required (Altroff et al 2001).

Statistical analysis

The cell functional data obtained are expressed as the means ± standard deviation (s.d.) of four replicates. Statistical analysis of the effects of increasing concentrations of immobilised ligand (FN, RGDS and polypeptide) on cell adhesion was performed using Friedman's (non-parametric) test. Statistical analysis of the inhibition of cell adhesion for increasing concentrations of soluble ligand was performed using the Mann–Whitney test (non-parametric test for two unpaired groups). $P < 0.05$ denoted significance in all cases. All analyses were performed using GraphPad Prism ver. 4.1 (GraphPad Software, CA, USA).

Results and Discussion

Characterisation of the polypeptide construct

The polypeptide was obtained at a modest yield of ca. 5 mg L^{-1} culture following expression in *E. coli*, with purification proceeding to homogeneity (Figure 2). Mass spectrometry analysis of peptide fragments verified the amino acid composition of the polypeptide over its entire sequence (data not shown). Running the polypeptide sample on the calibrated Superdex 75 HR10/30 column gave an estimated M_r for the tetramer of 39.5 kDa (Table 1, theoretical M_r 35.7 kDa). The discrepancy between the estimated and theoretical M_r is not unusual (Cabre et al 1989). The difference in M_r may also have arisen as a consequence of the predicted irregular structure of the tetramer extending its elution time in relation to elution times for the globular proteins used in the calibration.

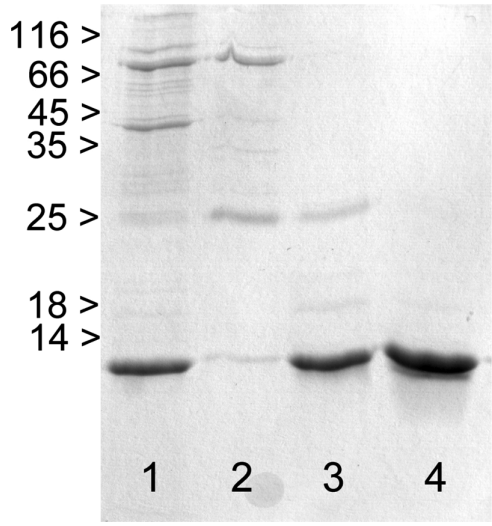

Figure 2 15% SDS-acrylamide gel showing polypeptide fractions following affinity chromatography (lane 1) and subsequent removal of impurities by size-exclusion chromatography (lanes 2 and 3) to yield purified polypeptide (lane 4). Position of Fermentas molecular weight markers (kDa) are shown on the left. Note, in SDS the polypeptide runs with an M_r corresponding to the single peptide chain.

Table 1 Estimation of the M_r of the polypeptide by size exclusion chromatography

Protein	Approx. M_r (kDa)	Elution vol. (V_e) (mL)	$K_{av} = (V_e/V_o)/(CV/V_o)$
HSA	66.0	9.10	0.083
Ovalbumin	45.0	9.68	0.119
FIII9–10	21.5	11.70	0.243
Myoglobin	17.0	12.22	0.275
FIII10	11.5	13.54	0.356
Polypeptide	39.5[a]	10.20	0.151
	7.1[b]	14.60	0.421

V_o, void volume; CV, column volume; [a,b]calculated from the K_{av} values corresponding to the early and late eluting peaks in the chromatogram, respectively; by regression analysis of data, the R-squared value was 0.99.

For a column volume of 25 mL, the theoretical dilution of the polypeptide injected (0.8 mM, 50 μL) was 5000×, giving an elution concentration of 0.16 μM. Along with the early elution peak corresponding to the tetrameric polypeptide, a later, broader peak of lower intensity was observed corresponding to a estimated M_r of 7.1 kDa (Table 1). This late peak most likely represented the monomeric polypeptide (the theoretical M_r being 8.9 kDa), the broadness of the peak probably giving rise to the error in MW calculation. Thus, there appeared to be evidence for dissociation of the tetramer during column elution at concentrations around 0.16 μM.

The CD spectrum for the purified polypeptide showed a strong minima at 208 nm with positive ellipticity peaking at 190 nm (Figure 3). The spectrum is composite with structural contributions from β-sheet to partial α-helix

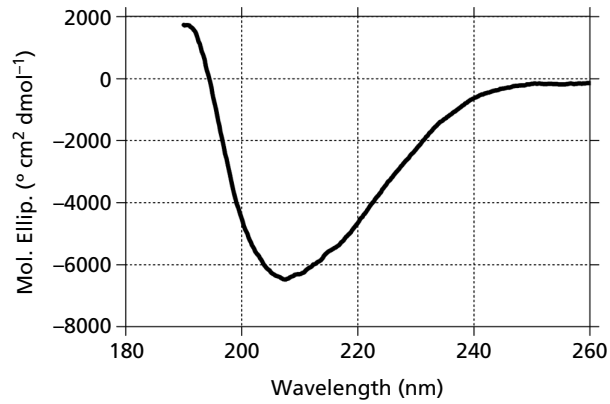

Figure 3 CD spectrum in the peptide region acquired for the polypeptide in phosphate buffer.

and random coil. Of the 82 residues (Met^{1}–Ser^{82}, Figure 1), 30 were derived from the β-sheet proteins, IgG and FN, 36 were derived from tetrabrachion and the remaining 16 comprised the N-terminal affinity tag with no assignable secondary structure. Therefore, the CD spectrum is qualitatively consistent with theoretical predictions for the polypeptide. Very similar CD spectra are observed for mixed secondary structures involving coiled coil-protein ligand constructs (Ahrens et al 2002). These data provide evidence that the polypeptide adopted a secondary structure facilitating self-assembly in solution to form the desired tetrameric RGD ligand.

Functional analysis of the polypeptide

HeLa cells and L929 fibroblast cells both adhered to surfaces coated with FN in the nanomolar range and RGDS in the millimolar range (Figure 4), as expected from previous data for integrin-mediated adhesion to FN and FIII 10 (Altroff et al 2001). Cell binding was verified to occur via interaction with the RGD motif since almost complete attenuation of cell adhesion was observed for the control polypeptide harbouring the RGE motif (Figure 5). For surfaces coated with $\leq 0.1\,\mu$M RGD-polypeptide, HeLa cells showed a weaker binding response than for surfaces coated with FN at an equivalent concentration (Figure 4A). However, above this concentration, HeLa cell adhesion to polypeptide-coated surfaces was stronger than for FN-coated surfaces, rising to around a 2-fold greater adhesion. L929 fibroblasts adhered better to surfaces coated with the polypeptide than either FN or RGDS peptide over all concentrations tested (Figure 4B). Around a 1.5- to 2-fold greater adhesion response was observed for polypeptide-coated surfaces over FN-coated surfaces at equivalent concentrations of 0.1–0.5 μM. Comparison of the three groups (FN, RGDS and polypeptide) by Friedman's test for Hela and L929 cell adhesion gave P values < 0.0001 (i.e., the means of the groups were significantly different). Cell adhesion to surfaces not coated with ligand, but BSA-blocked, was almost zero (Figure 4), showing show that non-specific cell adhesion was minimal.

Greater cell adhesion on surfaces coated with the polypeptide, in comparison to random monovalent ligand distributions for RGDS peptide and random displays for adsorbed FN, is consistent with polyvalent binding between integrin receptors and clustered RGD ligands (Maheshwari et al 2000). Although it cannot be directly proven that the peptide remained in a tetrameric state upon surface adsorption, the data are consistent with a clustered RGD ligand display for the adsorbed polypeptide. The difference in the cell adhesion profiles between HeLa and L929 cells is likely to be due to the different complement of integrin subtypes expressed by epithelial and fibroblast cell lines (Dzamba et al 2001).

The apparent sigmoidal curve for cell adhesion to the polypeptide possibly reports the dissociation constant, K_d, for tetrameric polypeptide assembly: the increase in cell adhesion occurring for coating concentrations of polypeptide in the 0.01–0.5 μM range (Figure 4). Thus, at concentrations

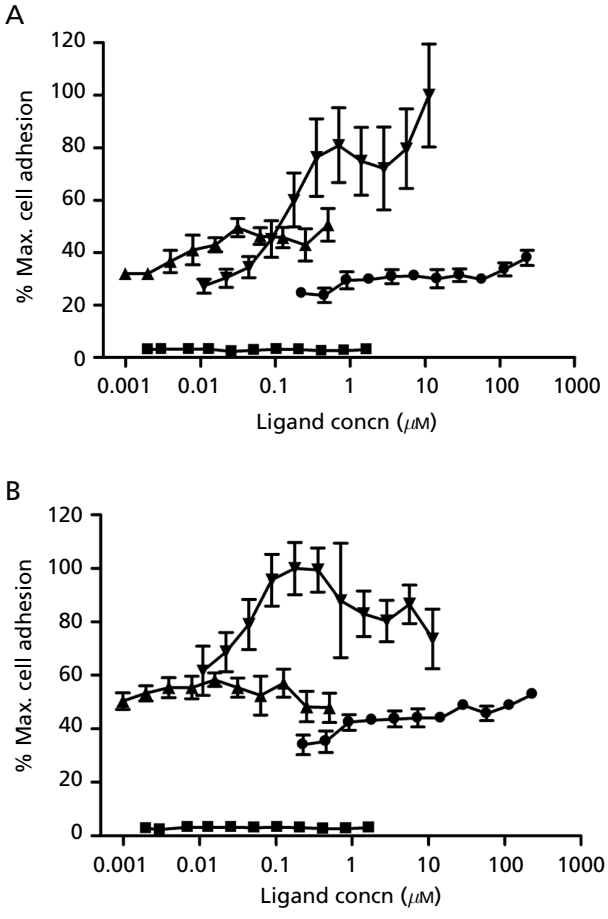

Figure 4 HeLa cell adhesion data (A) and L929 fibroblast adhesion data (B) for surfaces coated with FN (▲), RGDS (●), polypeptide (▼) and BSA (■). Error bars represent the sample s.d. (and are smaller than the symbols in the case of BSA).

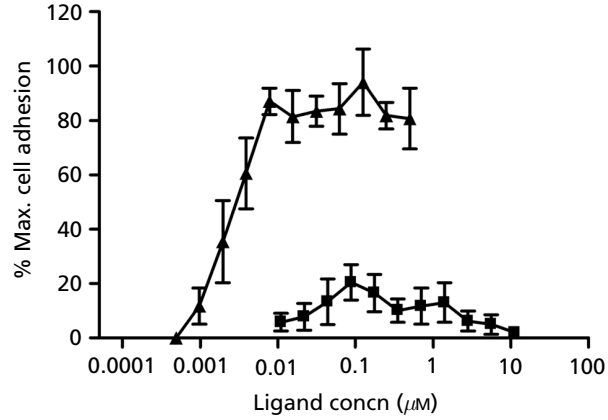

Figure 5 HeLa cell adhesion data for surfaces coated with the control (non-binding) polypeptide harbouring the RGE motif in place of RGD (■), in comparison with FN-coated surfaces (▲). Error bars represent the sample s.d.

above 0.5 μM the polypeptide existed as a stable tetramer, but at concentrations $< 0.5\,\mu$M began to dissociate with cell adhesion at low concentrations equivalent to the RGDS peptide. The apparent stability of the tetrameric polypeptide at concentrations to approx. 0.5 μM is in agreement with biophysical data for coiled coils, demonstrating their stability at concentrations $< 10\,\mu$M (Harbury et al 1998), although exact K_d values cannot easily be assigned (Thomas et al 1997). Moreover, the approximate K_d suggested from the cell adhesion data is in agreement with the approximate K_d determined from the size exclusion chromatography data (above).

Interestingly, L929 fibroblasts demonstrated a peak binding response to polypeptide around 0.2 μM, suggesting that at this average RGD density of 3×10^5 ligands/μm^2 a maximum number of integrin receptors were occupied by ligand. This value corresponds well with the minimal ligand density calculated for polymeric RGD clusters of five (10^5 ligands/μm^2) yielding near-maximum fraction cell adherence and cell migration speed (Maheshwari et al 2000). It is unlikely that high concentrations of polypeptide adsorbed less efficiently than low concentrations because the fraction of adhered HeLa cells continued to rise, although a small peak was seen for cell adhesion to surfaces coated with 1.0 μM polypeptide.

Only a modest improvement for HeLa cell and fibroblast cell adhesion to FN over RGDS peptide was observed. Cell adhesion to FN is generally considered to be stronger than to RGD due to the involvement of the FIII 9 synergy site which allows maximal binding to $\alpha5\beta1$ integrin (Aota et al 1994). However, this is only true when $\alpha5\beta1$ integrin binding predominates, since $\alpha v\beta3$ integrin maximally binds RGD (Pedchenko et al 2004). Also, for mixed $\alpha v\beta3$ and $\alpha5\beta1$ integrin populations, $\alpha v\beta3$ binding is favoured over $\alpha5\beta1$ binding on account of peptide conformational restriction (Massia & Hubbell 1991). Therefore, the HeLa cell and fibroblast cell adhesion profiles to FN and RGDS peptide are most likely to be accounted for by the mixed integrin populations known to be expressed by these cell types.

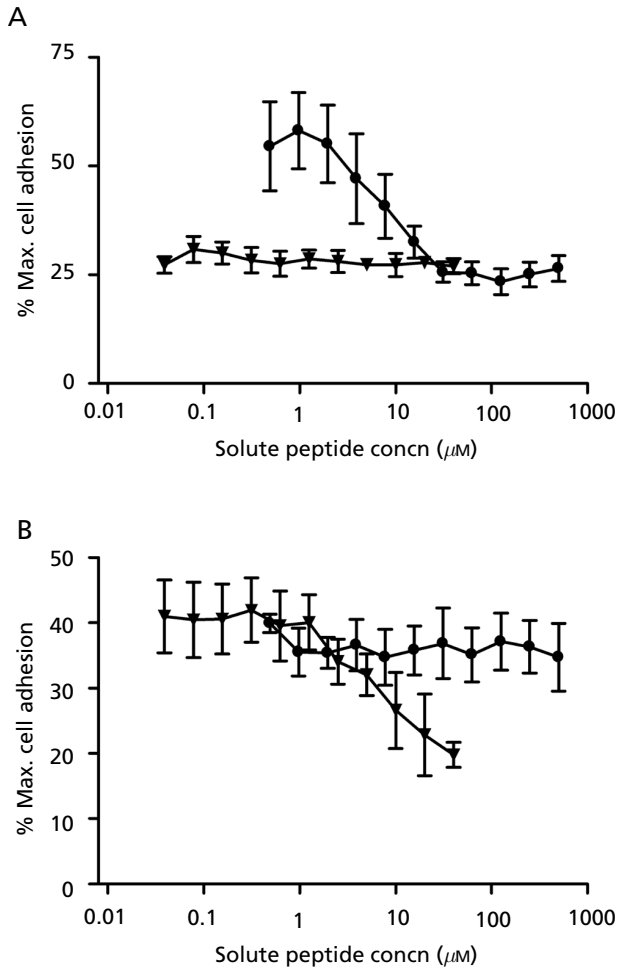

Figure 6 Inhibition of HeLa cell (A) and L929 fibroblast (B) adhesion to 0.05 μM FN-coated surfaces by RGDS (●) and polypeptide (▼). Adhesion is expressed as the percentage of the respective cell adhesion maximum in Figure 4. Error bars represent the sample s.d.

Inhibition of cell adhesion assays

In these assays, the extent of inhibition of cell adhesion to FN-coated plates was tested by prior binding of the ligand (polypeptide or RGDS) to cell surface integrin receptors. Conformational changes, which are commonly reported to occur upon adsorption of proteins/peptides to plastic surfaces, were therefore negated. Adhesion of HeLa cells was inhibited by RGDS only at concentrations $> 1.0\,\mu$M, and was strongly concentration dependent (Figure 6A). In contrast, micromolar to nanomolar concentrations of the polypeptide inhibited HeLa cell adhesion to approx. 40% of the HeLa cell adhesion response to surfaces coated with 0.05 μM FN (Figure 6A, cf. Figure 4A). For L929 fibroblasts, cell adhesion was only weakly inhibited by RGDS peptide to around 70% the level of adhesion to 0.05 μM FN (Figure 6B). A similar level of inhibition of fibroblast adhesion was observed for the polypeptide at concentrations $< 0.5\,\mu$M, but above this concentration cell adhesion decreased in a concentration-dependent manner to approx. 40% of the cell adhesion response to 0.05 μM FN (Figure 6B, cf. Figure 4B). Comparison of the two groups by the Mann–Whitney test for Hela and L929 cells gave P values < 0.01 for the 2–20 μM solute concentration region (i.e., the means of the groups were significantly different).

Inhibition of cell adhesion to FN-coated surfaces by polypeptide and RGDS provides evidence for their binding to integrin receptors, also demonstrated by the RGE polypeptide mutant (Figure 5). The greater inhibition of FN-mediated cell adhesion by polypeptide over RGDS at equivalent concentrations implies a higher integrin binding affinity for the polypeptide via polyvalent interaction. This is similar to

the observation that cell adhesion is enhanced through clustering of RGD ligand even though the average ligand density remains the same (Koo et al 2002). Further, mathematical modelling of integrin–ligand binding suggested that integrin occupancy for clustered ligand is greater than that for monovalent ligand and also described cooperativity between neighbouring integrin–ligand complexes, locally increasing binding affinity (Irvine et al 2002).

It should noted that interpretation of the curves observed for the inhibition of cell adhesion assays are complicated by the relative affinities of the integrin receptor population to the soluble ligand versus surface immobilised FN. The absence of a typical dose–response curve (i.e., little change in cell adhesion over a range of solute ligand concentrations) is not unusual. This may suggest incomplete inhibition or low affinity binding of ligand to specific integrin subtypes (e.g. integrin $\alpha 5\beta 1$ requires the FN synergy site in addition to RGD). This is observed in similar assays in our previous data (Altroff et al 2001).

Conclusions

To the best of our knowledge, this is the first report to describe the use of a right-handed tetrameric coiled coil motif to present a peptide ligand in a polyvalent manner. Extending the N- and C-termini of the coiled coil with unstructured peptides did not appear to have perturbed the propensity of the coiled coil to tetramerise or become less stable than the native tetrabrachion coiled coil. Further work will involve characterisation of the dissociation constant of the tetrameric polypeptide, such as determined by analytical ultracentrifugation or dilution isothermal calorimetry. Our data suggest a polyvalent interaction between integrin receptors and the polypeptide. Although we cannot assume that each arm (hinge-RGD) of the polypeptide tetramer bound an integrin receptor, given the cell data, steric hindrance between neighbouring integrins on polyvalent binding to the polypeptide does appear to have been adequately addressed via the spacer (the IgG-like hinge). Therefore, the polypeptide provides a template whereby protein ligands could be cloned in place of RGD to select binding to specific integrin subtypes. This may be of use in the synthesis of novel cell scaffolds. Such protein ligand substitutions could not be envisaged to be incorporated into the synthetic route for polymer-RGD combs (Maheshwari et al 2000; Koo et al 2002). Likewise, synthetic polymers presenting isolated RGD and synergy site peptides (Mardilovich & Kokkoli 2004) may have proven problematic because of the spatially conserved fibronectin binding sites (Grant et al 1997; Altroff et al 2004). In conclusion, we have designed a novel polypeptide that will be of interest to the development of targeted gene delivery vehicles and cell adhesive surfaces for tissue engineering.

References

Ahrens, T., Pertz, O., Haussinger, D., Fauser, C., Schulthess, T., Engel, J. (2002) Analysis of heterophilic and homophilic interactions of cadherins using the c-Jun/c-Fos dimerization domains. *J. Biol. Chem.* **277**: 19455–19460

Altroff, H., van der Walle, C. F., Asselin, J., Fairless, R., Campbell, I. D., Mardon, H. J. (2001) The eighth FIII domain of human fibronectin promotes integrin alpha5beta1 binding via stabilization of the ninth FIII domain. *J. Biol. Chem.* **276**: 38885–38892

Altroff, H., Schlinkert, R., van der Walle, C. F., Bernini, A., Campbell, I. D., Werner, J. M., Mardon, H. J. (2004) Interdomain tilt angle determines integrin-dependent function of the ninth and tenth FIII domains of human fibronectin. *J. Biol. Chem.* **279**: 55995–56003

Aota, S., Nomizu, M., Yamada, K. M. (1994) The short amino acid sequence Pro-His-Ser-Arg-Asn in human fibronectin enhances cell-adhesive function. *J. Biol. Chem.* **269**: 24756–24761

Cabre, F., Canela, E. I., Canela, M. A. (1989) Accuracy and precision in the determination of Stokes radii and molecular masses of proteins by gel filtration chromatography. *J. Chromatogr.* **472**: 347–356

Carman, C. V., Springer, T. A. (2003) Integrin avidity regulation: are changes in affinity and conformation underemphasized? *Curr. Opin. Cell Biol.* **15**: 547–556

Choquet, D., Felsenfeld, D. P., Sheetz, M. P. (1997) Extracellular matrix rigidity causes strengthening of integrin-cytoskeleton linkages. *Cell* **88**: 39–48

Dzamba, B. J., Bolton, M. A., Desimone, D. W. (2001) The integrin family of cell adhesion molecules. In: Bekerle, M. C. (ed.) *Cell adhesion*. Oxford University Press Inc., New York, pp 100–136

Fortunati, E., Ehlert, E., van Loo, N. D., Wyman, C., Eble, J. A., Grosveld, F., Scholte, B. J. (2000) A multi-domain protein for beta1 integrin-targeted DNA delivery. *Gene Ther.* **7**: 1505–1515

Grant, R. P., Spitzfaden, C., Altroff, H., Campbell, I. D., Mardon, H. J. (1997) Structural requirements for biological activity of the ninth and tenth FIII domains of human fibronectin. *J. Biol. Chem.* **272**: 6159–6166

Harbottle, R. P., Cooper, R. G., Hart, S. L., Ladhoff, A., McKay, T., Knight, A. M., Wagner, E., Miller, A. D., Coutelle, C. (1998) An RGD-oligolysine peptide: a prototype construct for integrin-mediated gene delivery. *Hum. Gene Ther.* **9**: 1037–1047

Harbury, P. B., Plecs, J. J., Tidor, B., Alber, T., Kim, P. S. (1998) High-resolution protein design with backbone freedom. *Science* **282**: 1462–1467

Harris, L. J., Larson, S. B., Hasel, K. W., McPherson, A. (1997) Refined structure of an intact IgG2a monoclonal antibody. *Biochemistry* **36**: 1581–1597

Humphries, M. J. (2000) Integrin structure. *Biochem. Soc. Trans.* **28**: 311–339

Ingham, K. C., Brew, S. A., Huff, S., Litvinovich, S. V. (1997) Cryptic self-association sites in type III modules of fibronectin. *J. Biol. Chem.* **272**: 1718–1724

Irvine, D. J., Hue, K. A., Mayes, A. M., Griffith, L. G. (2002) Simulations of cell-surface integrin binding to nanoscale-clustered adhesion ligands. *Biophys. J.* **82**: 120–132

Koo, L. Y., Irvine, D. J., Mayes, A. M., Lauffenburger, D. A., Griffith, L. G. (2002) Co-regulation of cell adhesion by nanoscale RGD organization and mechanical stimulus. *J. Cell Sci.* **115**: 1423–1433

Kunath, K., Merdan, T., Hegener, O., Haberlein, H., Kissel, T. (2003) Integrin targeting using RGD-PEI conjugates for in vitro gene transfer. *J. Gene Med.* **5**: 588–599

Maheshwari, G., Brown, G., Lauffenburger, D. A., Wells, A., Griffith, L. G. (2000) Cell adhesion and motility depend on nanoscale RGD clustering. *J. Cell Sci.* **113**: 1677–1686

Mardilovich, A., Kokkoli, E. (2004) Biomimetic peptide-amphiphiles for functional biomaterials: the role of GRGDSP and PHSRN. *Biomacromolecules* **5**: 950–957

Massia, S. P., Hubbell, J. A. (1991) An RGD spacing of 440 nm is sufficient for integrin alpha V beta 3-mediated fibroblast spreading and 140 nm for focal contact and stress fiber formation. *J. Cell Biol.* **114**: 1089–1100

Michaelsen, T. E., Frangione, B., Franklin, E. C. (1977) Primary structure of the hinge region of human IgG3. Probable quadruplication of a 15-amino acid residue basic unit. *J. Biol. Chem.* **252**: 883–889

Ohashi, T., Kiehart, D. P., Erickson, H. P. (1999) Dynamics and elasticity of the fibronectin matrix in living cell culture visualized by fibronectin-green fluorescent protein. *Proc. Natl Acad. Sci. USA* **96**: 2153–2158

Pedchenko, V., Zent, R., Hudson, B. G. (2004) Alpha(v)beta3 and alpha(v)beta5 integrins bind both the proximal RGD site and non-RGD motifs within noncollagenous (NC1) domain of the alpha3 chain of type IV collagen: implication for the mechanism of endothelia cell adhesion. *J. Biol. Chem.* **279**: 2772–2780

Pelham, R. J., Wang, Y. (1997) Cell locomotion and focal adhesions are regulated by substrate flexibility. *Proc. Natl Acad. Sci. USA* **94**: 13661–13665

Peters, J., Nitsch, M., Kuhlmorgen, B., Golbik, R., Lupas, A., Kellermann, J., Engelhardt, H., Pfander, J. P., Muller, S., Goldie, K., et al. (1995) Tetrabrachion: a filamentous archaebacterial surface protein assembly of unusual structure and extreme stability. *J. Mol. Biol.* **245**: 385–401

Pierschbacher, M. D., Ruoslahti, E. (1984) Cell attachment activity of fibronectin can be duplicated by small synthetic fragments of the molecule. *Nature* **309**: 30–33

Prodromou, C., Pearl, L. H. (1992) Recursive PCR: a novel technique for total gene synthesis. *Protein Eng.* **5**: 827–829

Rowley, J. A., Madlambayan, G., Mooney, D. J. (1999) Alginate hydrogels as synthetic extracellular matrix materials. *Biomaterials* **20**: 45–53

Stetefeld, J., Jenny, M., Schulthess, T., Landwehr, R., Engel, J., Kammerer, R. A. (2000) Crystal structure of a naturally occurring parallel right-handed coiled coil tetramer. *Nat. Struct. Biol.* **7**: 772–776

Tan, W., Krishnaraj, R., Desai, T. A. (2001) Evaluation of nanostructured composite collagen-chitosan matrices for tissue engineering. *Tissue Eng.* **7**: 203–210

Thomas, R. M., Zampieri, A., Jumel, K., Harding, S. E. (1997) A trimeric, alpha-helical, coiled coil peptide: association stoichiometry and interaction strength by analytical ultracentrifugation. *Eur. Biophys. J.* **25**: 405–410

Yang, X. B., Roach, H. I., Clarke, N. M. P., Howdle, S. M., Quirk, R., Shakesheff, K. M., Oreffo, R. O. C. (2001) Human osteoprogenitor growth and differentiation on synthetic biodegradable structures after surface modification. *Bone* **29**: 523–531